

Microscopic theory of the lattice dynamics of hcp rare-earth metals*

J. C. Upadhyaya[†]

Francis Bitter National Magnet Laboratory, Massachusetts Institute of Technology, Cambridge, Massachusetts 02139

A. O. E. Animalu

Lincoln Laboratory, Massachusetts Institute of Technology, Lexington, Massachusetts 02173

(Received 7 September 1976)

A microscopic theory of the lattice dynamics of the rare-earth metals based on the model-potential method is developed and applied to the hexagonal close-packed metals, Tb and Ho. The electron-phonon interaction is represented in the rigid-ion approximation by a rare-earth-metal model potential (REMMP) of the Heine-Abarenkov-Animalu type which incorporates formally the s - f hybridization in the energy bands of the lanthanides through an $l = 3$ model-potential well depth of the resonance form, $A_3(E) \propto 1/2 W_f/(E_f - E)$, where W_f and E_f are, respectively, the width and the position of the narrow f band. Physical effects due to the nonlocality of the REMMP, spin-orbit coupling, local-field corrections, and three-body forces are investigated but only the nonlocality of the REMMP was included explicitly in the numerical calculation. Calculated phonon dispersion curves for Tb and Ho are in reasonable agreement with the experimental data of Houmann and Nicklow and of Nicklow *et al.* This work represents a successful completion of the program of extending the pseudopotential and model-potential methods to all metals throughout the Periodic Table.

I. INTRODUCTION

Recently considerable progress has been made in the microscopic theory of the lattice dynamics of the transition metals by using the transition-metal model potential (TMMP) proposed by one of us¹ to represent the electron-phonon interaction. As in the microscopic theory of the lattice dynamics of the simple metals, based on the self-consistent field, Born-Oppenheimer, and harmonic approximations, one sets up a dispersion relation for phonons in a crystal of the form

$$[M\omega^2 \delta_{\alpha\beta} \delta_{\kappa\kappa'} - D_{\alpha\beta}(\vec{q}; \kappa\kappa')] e_{\beta}^s(\vec{q}) = 0 \quad (\alpha = 1, 2, 3), \quad (1)$$

where \vec{q} is the phonon wave vector restricted to the first Brillouin zone; $e_{\beta}^s(\vec{q})$ is the β component ($\beta = 1, 2, 3$) of the unit polarization vector, with (longitudinal and transverse) polarization index s ; M is the mass of the ions, and

$$D_{\alpha\beta} \equiv D_{\alpha\beta}^C + D_{\alpha\beta}^R + D_{\alpha\beta}^E \quad (2)$$

defines the dynamical matrix, comprised of three contributions, viz. the Coulombic ($D_{\alpha\beta}^C$), the repulsive core-core ($D_{\alpha\beta}^R$), and the electronic band-structure ($D_{\alpha\beta}^E$) contributions. For the common metallic structures, face-centered cubic (fcc), body-centered cubic (bcc), and hexagonal close packed (hcp), one calculates the Coulombic and the repulsive (Born-Mayer) contributions by standard techniques. For the electronic band-structure contribution, however, one needs to construct the electron-phonon interaction which, in the rigid-ion model, is determined by the pseudopotential or model potential carried by the vibrating ions. Our objective in this paper is to extend this approach

to the rare-earth metals, in particular, the hcp metals of the lanthanide series.

Animalu² and Khanna *et al.*³ have used the local form of the TMMP in the calculation of the phonon dispersion curves in the fcc transition metals with a measure of success. A similar approach using free-electron (Lindhard) dielectric function was less successful for the bcc transition metals. Subsequently, Oli and Animalu⁴ reformulated the lattice dynamics of the transition metals taking into account the s - d hybridization effects and local-field corrections to the free-electron dielectric function in the framework of a nonlocal TMMP theory: the formalism was applied to the bcc transition metals, vanadium⁴ and niobium,⁵ and reasonably good quantitative agreement between experimental and computed phonon dispersion curves was obtained. Using another formulation of the nonlocal theory due to Eschrig and Wonn,⁶ Kulshrestha and Upadhyaya⁷ have calculated the phonon dispersion curves for the hcp transition metals, Sc and Y: these authors reported large nonlocal effects and obtained good agreement with the experimental dispersion curves by treating the coefficient of the linear term in an expansion of the TMMP form factor near the Fermi surface as an adjustable parameter. In order to elucidate the source of the nonlocality in the TMMP, Maclin and Animalu⁸ recently performed a precise nonlocal dielectric screening of the TMMP in the resonance model using the single-plane-wave approximation and found that the screened nonlocal TMMP form factor of the Animalu-Heine type, $V(k, q)$ at $k = k_F$ did not differ significantly from the local TMMP approximation. Consequently, the large nonlocal ef-

fects reported by Kulshrestha and Upadhyaya⁷ appear to arise from the shift in energy due to ion-ion interaction via the polarization field of the conduction electrons which, in the random-phase approximation, is determined by the square of the pseudopotential or model-potential matrix elements and the Green's function summed over the occupied states in the Fermi distribution; or, in other words, the nonlocal effects are associated with the energy-wave-number characteristic function $G(q)$ and can be derived from first principles within a semilocal TMMP theory (see Sec. II B below).

In view of the above record of success based on the TMMP method, we wish in this paper to introduce a rare-earth-metal model potential (REMMP) and apply it to the lattice dynamics of the hcp rare-earth metals. The REMMP is presented in Sec. II A; the application to the calculation of the energy-wave-number characteristic in the framework of the Eschrig-Wonn nonlocal theory is developed in Sec. II B; and other corrections, in particular local-field corrections, spin-orbit coupling, and three-body forces are discussed in Sec. II C. Numerical results for Tb and Ho are presented and discussed in Sec. III; and conclusions are drawn in Sec. IV.

II. THEORY OF THE ELECTRONIC CONTRIBUTION

In this section, we wish to discuss the representation of the electronic contribution to the dynamical matrix for the phonon dispersion relation in a hcp metal by a rare-earth-metal model potential (REMMP) of the Heine-Abarenkov type. This is done in three parts: in Sec. II A, we describe a formal extension of the TMMP method to the lanthanide series; in Sec. II B, we derive the parameter in the Eschrig-Wonn nonlocal theory of the energy-wave-number characteristics from a semilocal REMMP approximation; and in Sec. II C, we discuss the various corrections due to local-fields, spin-orbit coupling, and three-body forces.

A. Rare-earth-metal model potential

The potential that an electron experiences in a vibrating lattice is related in the rigid-ion approximation, through the appropriate structure factor, to the pseudopotential or model potential associated with a single bare ion in the crystal. Following the procedure used in simple and transition-metal model-potential method, we represent the REMMP for a single ion by

$$V_M = \begin{cases} -\sum_{l=0}^{\infty} A_l(E) P_l & \text{for } r \leq R_M, \\ -z/r & \text{for } r > R_M, \end{cases} \quad (3)$$

where the model-potential well depths A_l are energy-dependent parameters to be determined from the atomic spectroscopic data in the spirit of the quantum-defect method, and all other notations have their usual meanings.¹

For the lanthanide group of rare-earth metals characterized by outer electronic configuration of the form $4f^n 5d^m 6s^2$ ($n=2, \dots, 14; m=1, 2$), and covering elements with atomic numbers from $Z=58$ (Ce) to $Z=71$ (Lu), the ions are predominantly trivalent ($z=3$) and the atomic spectroscopic term values⁹ (see Fig. 1) vary only slightly over the series. Electrons associated with the incomplete $4f$ shell are, like those associated with the incomplete d shells in the transition-group metals, virtual bound — a fact related to the s - f hybridization found in the energy bands of these metals calculated by the relativistic-augmented-plane-wave method.¹⁰ Spin-orbit coupling is also important for these high- Z metals.

In the spirit of the TMMP method in which s - d hybridization in the transition-metal energy bands is incorporated through an $l=2$ model well depth of the resonance form, $A_2(E) \propto (E_d - E)^{-1}$, we characterize s - f hybridization in the energy bands of the lanthanides in the REMMP by an $l=3$ model well depth of the resonance form

$$A_3(E) \propto \frac{1}{2} W_f / (E_f - E), \quad (4)$$

where E_f is the position and W_f the width of the f -band resonance. In practice, because of the similarity of the lanthanides to lanthanum (La), and the scarcity of the atomic spectroscopic data for the rare-earth metals in general, we shall use the model-potential parameters of La for $l=0, 1, 2$ (Ref. 1, Table I) as starting values for all the lanthanides. For convenience, these parameters for $l=0, 1, 2$ and our estimate for A_3 at $E=E_F$ derived from spectroscopic data are given explicitly

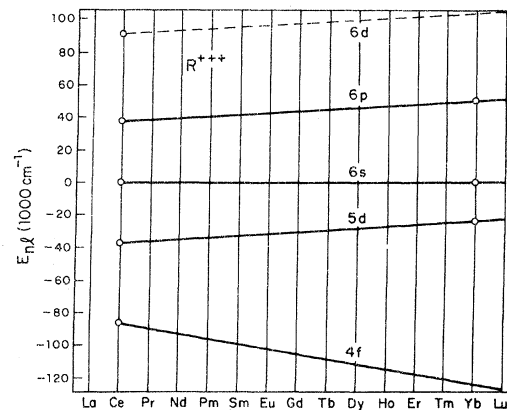


FIG. 1. Free-ion energy levels of the isoivalent sequence La^{3+} [La(IV)] (after Ref. 19).

TABLE I. Parameters of the model potential for La, Tb, and Ho. All quantities are in a.u. except $|E_c|$ (Ry).

Element	A_0	A_1	A_2	A_3	R_M	Ω	z	m^*	R_c	α_{eff}	$ E_c $
La	0.90	1.40	0.85	2.30	2.0	252.2	3	1.0	2.154	0.083	0.085
Tb	0.90	1.40	0.85	2.30	2.0	214.54	3	1.0	1.894	0.066	0.085
Ho	0.90	1.40	0.85	2.30	2.0	210.03	3	1.0	2.000	0.066	0.086

for La, Tb, and Ho in Tables I and II. Model-potential parameters for $l > 3$ need not be calculated if we optimize in the manner prescribed by Shaw¹¹ or use the standard approximation¹ of setting $A_l = C$ (for $l > 3$) to write the final REMMP in the form

$$V_M = \begin{cases} -C - (A_0 - C)P_0 - (A_1 - C)P_1 - (A_2 - C)P_2 \\ -(A_3 - C)P_3 \text{ for } r < R_M, \\ -z/r \text{ for } r > R_M. \end{cases} \quad (5)$$

Optimization consists of setting $C = z/r$ in this expression and allowing R_M to depend on l and E so that $A_l = z/R_M(l, E)$. For our present purpose, it suffices to put $C = z/R_M$ for fixed R_M in Eq. (5).

The screened REMMP form factor can be calculated in single plane-wave approximation by the procedure described in Ref. 8 for the TMMP. The result takes the form

$$\langle \vec{k} + \vec{q} | V | \vec{k} \rangle = B(q) / \epsilon(q) + F(\vec{k}, \vec{k} + \vec{q}) + I(F), \quad (6)$$

where $B(q)$ is the local part (including the orthogonalization and correlation corrections) and $F(\vec{k}, \vec{k} + \vec{q})$ the nonlocal part of the "bare" REMMP matrix element $\langle \vec{k} + \vec{q} | V_M | \vec{k} \rangle$; $I(F)$ is a complicated integral representing the screening field associated with the nonlocal part $F(\vec{k}, \vec{k} + \vec{q})$; and $\epsilon(q)$ is the

Hartree dielectric function, with appropriate modification for exchange and correlation.

B. Energy-wave-number characteristic function

We now proceed to describe the use of the REMMP form factor to represent the electronic contribution to the dynamical matrix for phonon dispersion relation in an hcp lattice.

The dynamical matrix for hcp structure containing two atoms per unit cell is a 6×6 matrix and can be expressed as

$$D(\vec{q}) = \begin{pmatrix} D(\vec{q}, \kappa\kappa) & D(\vec{q}, \kappa\kappa') \\ D^*(\vec{q}, \kappa\kappa') & D^*(\vec{q}, \kappa\kappa) \end{pmatrix}, \quad (7)$$

where the $D(\vec{q}, \kappa\kappa')$ are 3×3 submatrices, \vec{q} the phonon wave vector, and $\kappa, \kappa' = 1, 2$. As pointed out in Sec. I, the dynamical matrix is composed of Coulombic, repulsive, and electronic parts; the Ewald's θ -function transformation is used to calculate the Coulomb part from the relevant expression given elsewhere¹²; and the core-core repulsive part can be calculated from a Born-Mayer pair potential. The electronic parts are calculated by making use of the following expression:

$$D_{\alpha\beta}^E(\vec{q}, \kappa\kappa') = \frac{2z}{nM} \sum_{\vec{g}} (\vec{q} + \vec{g})_{\alpha} (\vec{q} + \vec{g})_{\beta} G_0(|\vec{q} + \vec{g}|) \exp(-i\vec{q} \cdot \vec{r}_{\kappa\kappa'}), \quad (8)$$

$$D_{\alpha\beta}^E(\vec{q}, \kappa\kappa) = \frac{2z}{nM} \sum_{\vec{g}} (\vec{q} + \vec{g})_{\alpha} (\vec{q} + \vec{g})_{\beta} G_0(|\vec{q} + \vec{g}|) - \sum_{\vec{g}}' \vec{g}_{\alpha} \vec{g}_{\beta} G_0(|\vec{g}|) F(\vec{r}).$$

Here, n is the number of ions per unit cell; and

$$F(\vec{r}) = \sum_{\kappa'} \cos(\vec{g} \cdot \vec{r}_{\kappa\kappa'}), \quad (9)$$

with $\vec{r}_{\kappa\kappa'} = \vec{r}_{\kappa} - \vec{r}_{\kappa'}$, and \vec{r}_{κ} and $\vec{r}_{\kappa'}$ being, respectively, the equilibrium positions of the two atoms in the unit cell. $G_0(q)$ is the (unnormalized) energy-wave-number characteristic function which depends on the "bare" pseudopotential or model-potential form factor $V_M(q)$ and is given in local model-potential approximation by the expression

$$G_0(q) = -\frac{\Omega_0 q^2}{8\pi z e^2} \frac{|V_M(q)|^2}{\epsilon(q)} \frac{\epsilon(q) - 1}{1 - f(q)}, \quad (10)$$

where $\epsilon(q)$ is the Hartree (free-electron) dielectric function with modification for exchange and correlation in the Hubbard-Sham or other analogous approximations.

TABLE II. Parameters used in the calculation of phonon frequencies: ν_p (10^{12} Hz); $k_F = (3\pi^2 z / \Omega)^{1/3}$ (a.u.); a and c are in Å and atomic mass M is in 10^{-24} g.

Element	ν_p	k_F	a	c	M
Tb	8.831	0.7453	3.59	5.696	264.336
Ho	8.745	0.7506	3.5773	5.6158	273.850

Now let us consider the nonlocal corrections to the energy-wave-number characteristic $G(q)$ in the manner proposed by Eschrig and Wonn.⁶ According to these authors, if one expands the form factor for k values near the Fermi wave number k_F and substitute in the standard expression¹³

$$G(q) \propto \sum_{\vec{k}} \frac{n(\vec{k}) - n(\vec{k} + \vec{q})}{E(\vec{k}) - E(\vec{k} + \vec{q})} \langle \vec{k} | V_M | \vec{k} + \vec{q} \rangle \langle \vec{k} + \vec{q} | V | \vec{k} \rangle, \quad (11)$$

the result may be written in the form

$$G(q) = G_0(q) [1 + a_q C(q)/D(q)], \quad (12)$$

where

$$C(q) = \frac{3}{2} z \left(1 + \eta^2 - \frac{(1 - \eta^2)^2}{2\eta} \ln \left| \frac{1 + \eta}{1 - \eta} \right| \right),$$

$$D(q) = \frac{3z}{2k_F^2} \left(1 + \frac{1 - \eta^2}{2\eta} \ln \left| \frac{1 + \eta}{1 - \eta} \right| \right),$$

$\eta = q/2k_F$, $G_0(q)$ being the energy-wave-number characteristic in the local screening approximation.

These and subsequent workers⁷ in the field of the lattice dynamics of hcp metals treated a_q as an arbitrary adjustable parameter in their calculations. It is possible, however, to determine this parameter in the framework of the nonlocal model-potential theory and hence exhibit its physical meaning. To this end, we use the local-screening approximation to write the screened model-potential form factor appearing in Eq. (11) as

$$\langle \vec{k} + \vec{q} | V | \vec{k} \rangle = [B(q) + F(\vec{k} + \vec{q}, \vec{k})]/\epsilon(q), \quad (13)$$

where $B(q)$ is the local part of the model potential (including the orthogonalization and correlation corrections), and $F(\vec{k} + \vec{q}, \vec{k})$ is the nonlocal \vec{k} - and E -dependent part. We also write

$$\langle \vec{k} | V_M | \vec{k} + \vec{q} \rangle = B(q) + F(\vec{k} + \vec{q}, \vec{k}). \quad (14)$$

Next, we expand the nonlocal part $F(\vec{k} + \vec{q}, \vec{k})$ as follows:

$$F(\vec{k} + \vec{q}, \vec{k}) = F(\vec{k}_F + \vec{q}, \vec{k}_F) + \left(\frac{\partial F}{\partial E} \right)_{E_F} (E - E_F), \quad (15)$$

where $\partial A_3/\partial E$ in this expression is obtained by differentiation of $A_3(E)$ defined by Eq. (21) below.

Finally, we substitute (13) and (15) in (11) and keep only terms of order $(\partial F/\partial E)_{E_F}$ to obtain the result in Eq. (12), with

$$a_q = \frac{2}{\langle \vec{k}_F + \vec{q} | V_M | \vec{k}_F \rangle} \left(\frac{\partial F}{\partial E} \right)_{E_F} \quad (16)$$

for $\langle \vec{k}_F + \vec{q} | V_M | \vec{k}_F \rangle \neq 0$.

In practice, a_q is not a smooth function of q , so that its treatment as an adjustable constant^{6,7} is unjustified. However, an exact treatment of the nonlocal effect is possible [though not practical, because of the large number of reciprocal-lattice vectors appearing in the summations in Eq. (8)]. In an exact treatment, instead of using the local approximation given by Eq. (13), we substitute the exact formula (6) in Eq. (11). Since $I(F)$ is a function of q only, we find from Eq. (11) that

$$G(q) \propto \sum_{\vec{k}} \frac{n(\vec{k}) - n(\vec{k} + \vec{q})}{E(\vec{k}) - E(\vec{k} + \vec{q})} [B(q) + F(\vec{k} + \vec{q}, \vec{k})] \left(\frac{B(q)}{\epsilon(q)} + F(\vec{k} + \vec{q}, \vec{k}) + I(F) \right) \quad (17)$$

does contain terms in $I(F)$ and $I(F^2)$, where

$$I(F) \propto \sum_{\vec{k}} \frac{n(\vec{k}) - n(\vec{k} + \vec{q})}{E(\vec{k}) - E(\vec{k} + \vec{q})} F(\vec{k} + \vec{q}, \vec{k}) \quad (18)$$

is given explicitly by [Ref. 8, Eq. (13)]:

$$I(F) = - \frac{32m^* [1 - f(q)] R_M^2}{\pi \Omega_0 Q^2 \epsilon(q)} \sum_{l=0}^3 (2l+1) L_l, \quad (19)$$

with

$$L_l = \int_{p \leq k_F} \frac{[A_l(E_p) - C] d\vec{p}}{(p^2 - |\vec{p} + \vec{q}|^2)} [p j_{l+1}(pR_M) j_l(|\vec{p} + \vec{q}|R_M) - |\vec{p} + \vec{q}| j_{l+1}(|\vec{p} + \vec{q}|R_M) j_l(pR_M)] P_l(\hat{p} \cdot \hat{q}), \quad (20)$$

$$A_l(E_p) = \begin{cases} A_l(E_F) + \left(\frac{\partial A_l}{\partial E} \right) (E_p - E_F) & \text{for } l=0, 1, 2, \\ \frac{A_3(E_F) |E_f - E_F|}{(E_f - E_p) + \frac{1}{2} iW_f} & \text{for } l=3, \end{cases} \quad (21)$$

$$E_p = \hbar^2 p^2 / 2m^*, \quad E_F = \hbar^2 k_F^2 / 2m^*, \quad E_f = \hbar^2 k_f^2 / 2m^*,$$

and $I(F^2)$ is defined similarly. The large contribution from nonlocality parameterized by a_q in Eq. (16) arises from $I(F^2)$ rather than from $I(F)$: this explains why nonlocality may be important in $G(q)$ but not in $\langle \vec{k} + \vec{q} | V | \vec{k} \rangle$ itself, as suggested in Sec. I. Our numerical calculations indicate that a constant a_q of order -1.0 gives a suitable approximation of

the exact formula (17) by the Eschrig-Wonn expression (12), for Tb and Ho. We accordingly treated a_q as an adjustable parameter to give a reasonable fit of the observed phonon dispersion curves in view of the fact that the available spectroscopic data were not sufficient to determine the $\partial A_l/\partial E$ for the relevant values of l .

C. Other corrections

We turn finally to other corrections to the electronic part of the dynamical matrix which are of interest for the hcp rare-earth metals. There are three corrections of significance, viz. spin-orbit coupling, local-field corrections, and three-body forces.

First, let us discuss spin-orbit coupling. Since we are dealing with elements of high atomic num-

ber, we expect spin-orbit coupling to be important. Inclusion of spin-orbit coupling in the model-potential scheme can be accomplished (see Ref. 5) by the procedure described by Animalu¹⁴ for the simple metals. Since the contribution of the spin-orbit model potential V_{so} to the form factor is pure imaginary, it may be incorporated in Eq. (10) simply by replacing $|V_M(q)|^2$ by $[|V_M(q)|^2 + |V_{so}(q)|^2]$. Since the spectroscopic data for the lanthanides are scanty, we have made a quantitative estimate of this contribution using the data on La and found spin-orbit contribution to the lattice dynamics of the lanthanides to be negligible.

Next, let us consider the local-field corrections. Following the discussion given by Oli and Animalu⁴ for the cubic transition metals, we modify the electronic contribution to the dynamical matrix in hcp structure in the following way:

$$D_{\alpha\beta}(\vec{q}, \kappa\kappa') = \frac{2z}{nM} \sum_{\vec{g}} \sum_{\vec{g}'} (\vec{q} + \vec{g})_{\alpha} (\vec{q} + \vec{g}')_{\beta} G(\vec{q} + \vec{g}, \vec{q} + \vec{g}') \exp(+i\vec{g} \cdot \vec{r}_{\kappa}) \exp(-i\vec{g}' \cdot \vec{r}_{\kappa'}),$$

$$D_{\alpha\beta}(\vec{q}, \kappa\kappa') = \frac{2z}{nM} \left(\sum_{\vec{g}} \sum_{\vec{g}'} (\vec{q} + \vec{g})_{\alpha} (\vec{q} + \vec{g}')_{\beta} G(\vec{q} + \vec{g}, \vec{q} + \vec{g}') - \sum_{\vec{g}} \sum_{\vec{g}'}' \vec{g}_{\alpha} \vec{g}'_{\beta} G(\vec{g}, \vec{g}') F(\kappa) \right), \quad (22)$$

where

$$F(\kappa) = \frac{1}{2} [\exp(+i\vec{g} \cdot \vec{\kappa}) + \exp(-i\vec{g}' \cdot \vec{\kappa})],$$

$$G(\vec{q} + \vec{g}, \vec{q} + \vec{g}') = -(\Omega_0 |\vec{q} + \vec{g}|^2 / 8\pi z e^2) \chi(\vec{q} + \vec{g}, \vec{q} + \vec{g}') \\ \times V_M(\vec{q} + \vec{g}) \epsilon^{-1}(\vec{q} + \vec{g}, \vec{q} + \vec{g}') V_M(\vec{q} + \vec{g}'), \quad (23)$$

$$\chi(\vec{q} + \vec{g}, \vec{q} + \vec{g}') = [v(\vec{q} + \vec{g})]^{-1} [\delta_{\vec{g}, \vec{g}'} - \epsilon(\vec{q} + \vec{g}, \vec{q} + \vec{g}')],$$

$v(\vec{q} + \vec{g})$ being the Fourier transform of the electron-electron Coulomb interaction with appropriate modification for exchange and correlation. This involves the inverse dielectric matrix $\epsilon^{-1}(\vec{q} + \vec{g}, \vec{q} + \vec{g}')$ whose off-diagonal components are generated by the depletion hole arising from the energy dependence of the REMMP [cf. Ref. 4, Eq. (22)]. Estimate of this contribution is hampered by lack of enough atomic spectroscopic data required to evaluate the derivatives of the REMMP parameters dA_l/dE which also appear in the full nonlocal theory through Eq. (20).

Finally, we turn to the three-body forces. The experimental dispersion curves for Tb,¹⁵ and Ho,¹⁶ indicate that along ΓKM direction, the ordering of dispersion branches and the degeneracy at the K point are similar to those of hcp Be.^{17, 18} The analysis of Roy *et al.*¹⁷ suggests that these special features of the phonon spectrum of Be, and hence those of Tb and Ho, are a direct manifestation of

unpaired, i.e., three-body forces; this feature cannot be explained by a simple pseudopotential model based on second-order perturbation theory or by the modified axially symmetric model of deWames *et al.*¹⁹ with any number of adjustable parameters. Bertoni *et al.*²⁰ have shown, however, that the inclusion of third-order perturbation terms and hence three-body forces in the pseudopotential formalism was sufficient to explain these special features. We expect the approach of Bertoni *et al.*²⁰ which is based on the Heine-Abarenkov model potential for Be to be relevant in Tb and Ho. Unpaired forces are also introduced by the use of a nondiagonal dielectric matrix for screening, but no calculation exists in current literature. We have not included the unpaired forces in the present calculation.

III. NUMERICAL RESULTS AND DISCUSSION

We now proceed to present the numerical results based on the theory presented in Sec. II and to compare them with experimental phonon dispersion curves. Along the high-symmetry directions, ΓA , ΓM , and ΓKM corresponding, respectively, to the $[0001]$, $[01\bar{1}0]$, and $[11\bar{2}0]$ directions in the Brillouin zone, the secular equation (1) can be solved to determine the phonon frequencies ν from the following relations:

For the [001] symmetry direction ($q_x = q_y = 0$,
 $q_z = q$),

$$\omega^2(q) = D_{zz}(q, \kappa\kappa) \pm |D_{zz}(q, \kappa\kappa')|, \quad \text{LO and LA}, \quad (24)$$

$$\omega^2(q) = D_{xx}(q, \kappa\kappa) \pm |D_{xx}(q, \kappa\kappa')|, \quad \text{TO and TA}.$$

For the [01 $\bar{1}$ 0] symmetry direction ($q_x = q_z = 0$,
 $q_y = q$),

$$\omega^2(q) = D_{yy}(q, \kappa\kappa) \pm |D_{yy}(q, \kappa\kappa')|, \quad \text{LO and LA},$$

$$\omega^2(q) = D_{zz}(q, \kappa\kappa) \pm |D_{zz}(q, \kappa\kappa')|, \quad \text{TO}(\perp) \text{ and TA}(\perp), \quad (25)$$

$$\omega^2(q) = D_{xx}(q, \kappa\kappa) \pm |D_{xx}(q, \kappa\kappa')|, \quad \text{TO}(\parallel) \text{ and TA}(\parallel).$$

For the [11 $\bar{2}$ 0] symmetry direction ($q_y = q_z = 0$,
 $q_x = q$),

$$\omega^2(q) = D_{zz}(q, \kappa\kappa) \pm [D_{zz}^*(q, \kappa\kappa')D_{zz}(q, \kappa\kappa')]^{1/2}, \quad T_2 \text{ and } T_3,$$

$$\omega^2(q) = \frac{1}{2} (D_{xx}(q, \kappa\kappa) + \text{Re } D_{xx}(q, \kappa\kappa') + D_{yy}(q, \kappa\kappa) - \text{Re } D_{yy}(q, \kappa\kappa'))$$

$$\pm \{ [D_{xx}(q, \kappa\kappa) + \text{Re } D_{xx}(q, \kappa\kappa') - D_{yy}(q, \kappa\kappa) + \text{Re } D_{yy}(q, \kappa\kappa')]^2$$

$$+ 4[\text{Im } D_{xy}(q, \kappa\kappa) - \text{Im } D_{xy}(q, \kappa\kappa')]^2 \}^{1/2}, \quad T_1^+ \text{ and } T_1^-, \quad (26)$$

$$\omega^2(q) = \frac{1}{2} (D_{xx}(q, \kappa\kappa) - \text{Re } D_{xx}(q, \kappa\kappa') + D_{yy}(q, \kappa\kappa) + \text{Re } D_{yy}(q, \kappa\kappa'))$$

$$\pm \{ [D_{xx}(q, \kappa\kappa) - \text{Re } D_{xx}(q, \kappa\kappa') - D_{yy}(q, \kappa\kappa) - \text{Re } D_{yy}(q, \kappa\kappa')]^2$$

$$+ 4[\text{Im } D_{xy}(q, \kappa\kappa) + \text{Im } D_{xy}(q, \kappa\kappa')]^2 \}^{1/2}, \quad T_4 \text{ and } T_4^-.$$

TABLE III. Coulomb coefficients for Tb [units of $4\pi(ze)^2/M\Omega$]. Ω , the atomic volume per unit cell, equals $2\Omega_0$ (Ω_0 is the atomic volume), M is the ionic mass, z is the chemical valence, and e is the electronic charge.

[0001] direction									
q/q_{\max}	$D_{xx}(\vec{q}, \kappa\kappa)$	$D_{zz}(\vec{q}, \kappa\kappa)$	$D_{xx}(\vec{q}, \kappa\kappa')$	$D_{zz}(\vec{q}, \kappa\kappa')$					
0.2	0.052 14	1.895 50	-0.049 65	0.099 31					
0.4	0.051 97	1.895 83	-0.042 24	0.084 48					
0.6	0.051 76	1.896 28	-0.030 69	0.061 37					
0.8	0.051 58	1.896 63	-0.016 13	0.032 27					
1.00	0.051 52	1.896 78	0.0	0.0					
[01 $\bar{1}$ 0] direction									
q/q_{\max}	$D_{xx}(\vec{q}, \kappa\kappa)$	$D_{yy}(\vec{q}, \kappa\kappa)$	$D_{zz}(\vec{q}, \kappa\kappa)$	$D_{xx}(\vec{q}, \kappa\kappa')$		$D_{yy}(\vec{q}, \kappa\kappa')$		$D_{zz}(\vec{q}, \kappa\kappa')$	
				Re	Im	Re	Im	Re	Im
0.2	0.066 94	1.085 19	0.847 86	-0.053 86	0.031 49	0.891 93	-0.032 83	-0.838 07	0.001 34
0.4	0.105 69	1.165 63	0.728 67	-0.058 12	0.061 02	0.745 18	-0.071 82	-0.687 06	0.010 80
0.6	0.153 92	1.254 21	0.591 86	-0.063 05	0.086 09	0.552 41	-0.122 92	-0.489 37	0.036 83
0.8	0.193 23	1.317 84	0.488 84	-0.066 00	0.103 76	0.352 35	-0.191 80	-0.286 35	0.088 03
1.00	0.208 31	1.340 43	0.451 15	-0.064 45	0.111 63	0.163 72	-0.283 56	-0.099 27	0.171 94
[11 $\bar{2}$ 0] direction									
q/q_{\max}	$D_{xx}(\vec{q}, \kappa\kappa)$	$D_{yy}(\vec{q}, \kappa\kappa)$	$D_{zz}(\vec{q}, \kappa\kappa)$	$D_{xx}(\vec{q}, \kappa\kappa')$	$D_{yy}(\vec{q}, \kappa\kappa')$	$D_{zz}(\vec{q}, \kappa\kappa')$	$\text{Im } D_{xy}(\vec{q}, \kappa\kappa')$		
0.2	1.134 11	0.101 17	0.764 70	0.792 36	-0.058 17	-0.734 19	0.569 22		
0.4	1.185 15	0.281 27	0.533 57	0.481 11	-0.085 34	-0.395 78	0.122 27		
0.6	0.943 03	0.641 72	0.415 24	0.237 52	-0.154 91	-0.082 62	0.181 68		
0.67	0.794 82	0.796 40	0.408 76	0.188 95	-0.189 33	0.000 39	0.189 16		
0.8	0.471 22	1.103 66	0.425 11	0.139 32	-0.264 32	0.125 01	0.161 66		
1.0	0.208 31	1.340 43	0.451 16	0.128 90	-0.327 43	0.198 53	0.0		

TABLE IV. Coulomb coefficients for holmium [units of $4\pi(ze)^2/M\Omega$. Ω , the atomic volume per unit cell, equals $2\Omega_0$ (Ω_0 is the atomic volume), M is the ionic mass, z is the chemical valence, and e is the electronic charge.

[0001] direction									
q/q_{\max}	$D_{xx}(\vec{q}, \kappa\kappa)$	$D_{zz}(\vec{q}, \kappa\kappa)$	$D_{xx}(\vec{q}, \kappa\kappa')$	$D_{zz}(\vec{q}, \kappa\kappa')$					
0.2	0.054 71	1.890 34	-0.052 11	0.104 22					
0.4	0.054 52	1.890 75	-0.044 33	0.088 65					
0.6	0.054 28	1.891 21	-0.032 20	0.064 41					
0.8	0.054 09	1.891 65	-0.016 93	0.033 86					
1.0	0.054 09	1.891 65	0.0	0.0					
[0110] direction									
q/q_{\max}	$D_{xx}(\vec{q}, \kappa\kappa)$	$D_{yy}(\vec{q}, \kappa\kappa)$	$D_{zz}(\vec{q}, \kappa\kappa)$	$D_{xx}(\vec{q}, \kappa\kappa')$		$D_{yy}(\vec{q}, \kappa\kappa')$		$D_{zz}(\vec{q}, \kappa\kappa')$	
				Re	Im	Re	Im	Re	Im
0.2	0.069 37	1.086 35	0.844 26	-0.056 48	0.032 80	0.890 40	-0.034 16	-0.833 91	0.001 36
0.4	0.107 72	1.163 45	0.728 82	-0.060 83	0.063 54	0.745 94	-0.074 49	-0.685 11	0.010 95
0.6	0.155 46	1.248 55	0.595 97	-0.065 85	0.089 61	0.555 19	-0.126 89	-0.489 33	0.037 28
0.8	0.194 37	1.309 91	0.495 70	-0.068 80	0.108 00	0.355 94	-0.196 90	-0.287 14	0.088 90
1.0	0.209 30	1.331 71	0.458 98	-0.067 09	0.116 21	0.167 06	-0.289 36	-0.099 97	0.173 15
[1120] direction									
q/q_{\max}	$D_{xx}(\vec{q}, \kappa\kappa)$	$D_{yy}(\vec{q}, \kappa\kappa)$	$D_{zz}(\vec{q}, \kappa\kappa)$	$D_{xx}(\vec{q}, \kappa\kappa')$	$D_{yy}(\vec{q}, \kappa\kappa')$	$D_{zz}(\vec{q}, \kappa\kappa')$	$\text{Im}D_{xy}(\vec{q}, \kappa\kappa')$		
0.2	1.132 98	0.103 26	0.763 74	0.792 51	-0.060 89	-0.731 62	0.059 18		
0.4	1.179 17	0.281 58	0.539 24	0.484 86	-0.088 62	-0.396 25	0.126 49		
0.6	0.937 44	0.638 68	0.423 86	0.242 39	-0.159 37	-0.830 29	0.186 80		
0.67	0.790 43	0.792 00	0.417 54	0.193 91	-0.194 30	0.000 39	0.194 12		
0.9	0.469 77	1.096 70	0.433 51	0.144 44	-0.270 28	0.125 84	0.165 41		
1.0	0.209 30	1.331 71	0.458 98	0.134 19	-0.334 12	0.199 93	0.0		

where the “+” sign denotes the optical branches and the “-” sign the acoustic branches.

The Coulomb coefficients calculated from the expressions given in Ref. 12 are tabulated in Tables III and IV for Tb and Ho for the principal symmetry directions given in Eqs. (24)–(26). Since the parameters characterizing the Born-Mayer repulsive contribution are not available for the lanthanides, we have not included this contribution (typically 5%) in the calculated phonon dispersion curves. The electronic contribution is calculated in semilocal REMMP approximation using the expression for the form factor given in Appendix A, and $a_q = -1$ in Eq. (12) as discussed in Sec. II B.

Typical values of the phonon frequencies are tabulated for some branches in Tb in Table V; and

TABLE V. Phonon frequencies (units of 10^{12} Hz) of Tb for some branches.

q/q_{\max}	ΓA direction		ΓM direction		ΓKM direction	
	Δ_5	Δ_6	Σ_3^U	Σ_3^L	T_3	T_2
0.2	0.32	3.56	0.35	3.55	0.54	3.35
0.4	0.62	3.31	0.74	3.32	1.61	2.98
0.6	0.96	2.90	1.34	3.10	2.29	2.54
0.8	1.45	2.49	1.83	2.85	2.58	2.23
1.0	1.94	1.94	2.14	2.66	2.66	2.14

the complete phonon dispersion curves are displayed in Figs. 2–5, for Tb and Ho, and compared with experiments. The agreement between theory and experiment is only semiquantitative in view of the corrections due to local-fields and three-body forces which have been omitted in this calculation for the reasons given in Sec. II C. Although the results are sensitive to the value of a_q (treated here

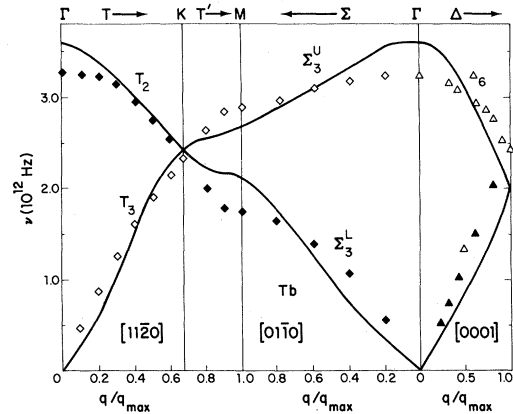


FIG. 2. Phonon dispersion in Tb: solid curves represent the calculations of the present work; $\diamond\triangle\blacktriangle$ experimental points of Houmann and Nicklow (Ref. 15).

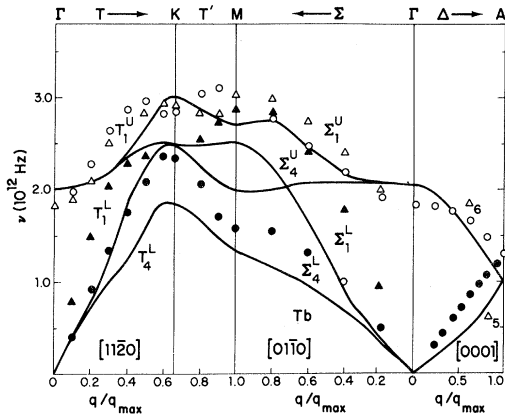


FIG. 3. Phonon dispersion in Tb: solid curves represent the calculations of the present work; $\circ\Delta\blacktriangle$ experimental points of Houmann and Nicklow (Ref. 15).

as an adjustable parameter), they are quite stable up to 50% change in the value of $A_3(E_F)$ because of the small amplitude of the $l=3$ spherical Bessel function.

IV. CONCLUSION

In this paper, we have developed a microscopic theory of the lattice dynamics of the hcp rare-earth metals based on the Heine-Abarenkov-Animalu model-potential method. This work represents a successful completion of the model-potential program for *all* metals in the Periodic Table. It reassures us that the pseudopotential concept is applicable universally to simple, transition, and rare-earth metals provided some care is taken in

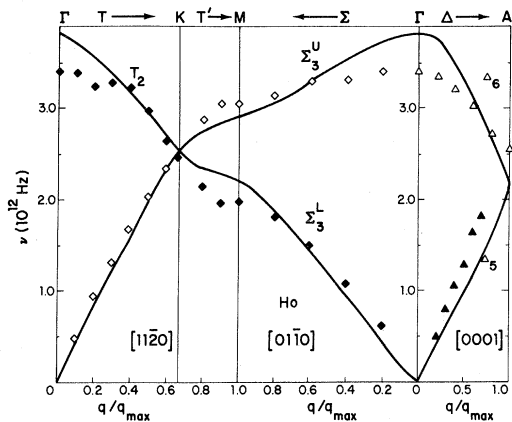


FIG. 4. Phonon dispersion in Ho: solid curves represent the calculations of present work; $\diamond\blacktriangle$ experimental points of Nicklow *et al.* (Ref. 16).

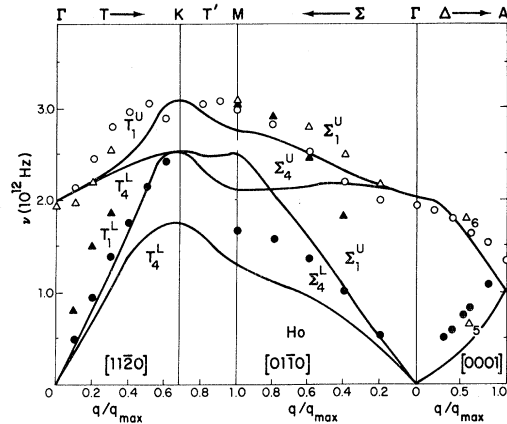


FIG. 5. Phonon dispersion in Ho: solid curves represent the calculations of the present work; $\circ\Delta\blacktriangle$ experimental points of Nicklow *et al.* (Ref. 16).

the treatment of the *d*-band resonance in the transition metals, and the *f*-band resonance in the rare-earth metals. However, certain problems remain to be solved. For example, an internally consistent treatment of the chemical valence and the incomplete shells of the transition and rare-earth metals is yet to be given: we expect such a treatment to lead to a model-potential theory of magnetism in metals. The resonance model, as presently represented in the TMMP and the REMMP, is an oversimplification of the complex structure of the *d* band and the *f* band in real metals; but it contains the essential ingredient required to investigate the physical effects of *s-d* and *s-f* hybridization in electronic properties. In spite of these problems, we feel that the microscopic theory of the electron-phonon interaction and the lattice dynamics of the transition and rare-earth metals presented thus far is reliable enough to permit a program to investigate a number of outstanding problems of the electronic properties of these metals, particularly superconductivity.

ACKNOWLEDGMENT

One of us (J.C.U.) wishes to thank the Francis Bitter National Magnet Laboratory for their hospitality and M.I.T. Lincoln Laboratory for making their computer facility available.

APPENDIX A

In this Appendix, we wish to give an explicit expression for the screened-model-potential form factor $V(q)$. In the local screening approximation

$$V(q) = V^b(q)/\epsilon(q), \quad (A1)$$

where

$$\begin{aligned} V^b(q) &= \langle \vec{k}_F + \vec{q} | V_M + V_{oc} + V_{cc} | \vec{k}_F \rangle \\ &\equiv F(\vec{k}_F, \vec{k}_F + \vec{q}) + B(q), \end{aligned} \quad (\text{A2})$$

say, V_M being the model potential defined by Eq. (5) and V_{oc}, V_{cc} the usual orthogonalization and correlation corrections.

In Eq. (A2),

$$B(q) = -\frac{8\pi C}{\Omega q^3} [\sin(qR_M) - qR_M \cos(qR_M)] - \frac{8\pi z}{\Omega q^2} \cos(qR_M) + \left(\frac{4\pi |E_c|}{\Omega q^3} - \frac{24\pi z \alpha_{\text{eff}}}{\Omega q^2 (qR_c)^3} \right) [\sin(qR_c) - qR_c \cos(qR_c)]. \quad (\text{A3})$$

For $|\vec{k}_F + \vec{q}| = k_F$,

$$\begin{aligned} F(\vec{k}_F, \vec{k}_F + \vec{q}) &= -4\pi\Omega^{-1}R_M^3(A_0 - C) \{ [j_0(x)]^2 - x^{-1} \cos(x)j_1(x) \} - 12\pi\Omega^{-1}R_M^3(A_1 - C) \\ &\quad \times \{ [j_1(x)]^2 - j_0(x)j_2(x) \} P_1(\cos\theta) - 20\pi\Omega^{-1}R_M^3(A_2 - C) \\ &\quad \times \{ [j_2(x)]^2 - j_1(x)j_3(x) \} P_2(\cos\theta) - 28\pi\Omega^{-1}R_M^3(A_3 - C) \{ [j_3(x)]^2 - j_2(x)j_4(x) \} P_3(\cos\theta), \end{aligned} \quad (\text{A4})$$

where $x = k_F R_M$, $\cos\theta = 1 - q^2/2k_F^2$; $C = z/R_M$;

$$P_1(\cos\theta) = \cos\theta, \quad P_2(\cos\theta) = \frac{1}{2}(3\cos^2\theta - 1), \quad P_3(\cos\theta) = \frac{1}{8}[5\cos^3\theta - 3\cos\theta];$$

$$j_0(x) = x^{-1} \sin x, \quad j_1(x) = x^{-2} \sin x - x^{-1} \cos x, \quad j_2(x) = (3x^{-3} - x^{-1}) \sin x - 3x^{-2} \cos x,$$

$$j_3(x) = 5x^{-4} j_2(x) - j_1(x), \quad j_4(x) = 7x^{-5} j_3(x) - j_2(x).$$

For $|\vec{k}_F + \vec{q}| \neq k_F$,

$$\begin{aligned} F(k_F, k_F + q) &= -\frac{8\pi R_M^3(A_0 - C)}{\Omega(x^2 - y^2)} [xj_1(x)j_0(y) - yj_1(y)j_0(x)] - \frac{24\pi R_M^3(A_1 - C)}{\Omega(x^2 - y^2)} \\ &\quad \times [xj_2(x)j_1(y) - yj_2(y)j_1(x)] P_1(\cos\theta') - \frac{40\pi R_M^3(A_2 - C)}{\Omega(x^2 - y^2)} [xj_3(x)j_2(y) - yj_3(y)j_2(x)] P_2(\cos\theta') \\ &\quad - \frac{56\pi R_M^3(A_3 - C)}{\Omega(x^2 - y^2)} [xj_4(x)j_3(y) - yj_4(y)j_3(x)] P_3(\cos\theta'), \end{aligned} \quad (\text{A5})$$

where

$$x = k_F R_M, \quad y = |\vec{k}_F + \vec{q}| R_M, \quad (\text{A6})$$

$$\cos\theta' = [x^2 + y^2 - (qR_M)^2] / 2xy.$$

The dielectric function $\epsilon(q)$ is given by

$$\epsilon(q) = 1 + [1 - f(q)](4\pi z e^{*2} / \Omega q^2) \chi(q/2k_F), \quad (\text{A7})$$

where

$$\chi(X) = \frac{3}{2} E_F \left[\frac{1}{2} + \frac{1}{4} \left(\frac{1 - X^2}{X} \right) \ln \left| \frac{1 + X}{1 - X} \right| \right], \quad (\text{A8})$$

$$E_F = \hbar^2 k_F^2 / 2m^*, \quad (\text{A9})$$

$$e^{*2} = (1 + \alpha_{\text{eff}}) e^2, \quad (\text{A10})$$

and

$$f(q) = q^2 / [2(q^2 + k_F^2 + k_s^2)]; \quad k_s^2 = 2k_F / \pi \text{ (a.u.)}. \quad (\text{A11})$$

The final answer obtained by inserting the numbers in Tables I and II into $V(q)$ is in Ry.

*Work sponsored by the Department of the Air Force.

†Visiting Scientist from the Dept. of Physics, Agra College, Agra, India.

¹A. O. E. Animalu, Phys. Rev. B **8**, 3542 (1973).

²A. O. E. Animalu, Phys. Rev. B **8**, 3555 (1973).

³S. N. Khanna, J. C. Upadhyaya, and Ashok Jain, Phys. Status Solidi B **65**, K25 (1974).

⁴B. A. Oli and A. O. E. Animalu, Phys. Rev. B **13**, 2398 (1976).

⁵B. A. Oli, Ph.D. thesis (MIT, 1976) (unpublished).

⁶H. Eschrig and H. Wonn, Phys. Status Solidi **40**, 163 (1970).

⁷O. P. Kulshrestha and J. C. Upadhyaya, Phys. Rev. B **13**, 1861 (1976).

⁸A. P. Maclin and A. O. E. Animalu, Phys. Rev. (to be published).

⁹G. H. Dieke, *Spectra and Energy Levels of Rare-Earth Ions in Crystals* (Interscience, New York, 1968), p. 52.

¹⁰T. L. Loucks, *Augmented Plane Wave Method* (Benjamin, New York, 1967), p. 73.

¹¹R. W. Shaw, Phys. Rev. **174**, 769 (1968).

¹²J. A. Reissland and Osman Ese, J. Phys. F **5**, 110 (1975).

¹³A. O. E. Animalu, Proc. R. Soc. A **294**, 376 (1966).

- ¹⁴A. O. E. Animalu, *Philos. Mag.* 13, 53 (1966).
- ¹⁵J. C. G. Houmann and R. M. Nicklow, *Phys. Rev. B* 1, 3943 (1970).
- ¹⁶R. M. Nicklow, N. Wakabayashi, and P. R. Vijayaraghavan, *Phys. Rev. B* 3, 1229 (1971).
- ¹⁷A. P. Roy, B. A. Dasannacharya, C. L. Thaper, and P. K. Iyengar, *Phys. Rev. Lett.* 30 906 (1973).
- ¹⁸J. C. Upadhyaya and R. P. Sharma, *Phys. Rev. B* 6, 2692 (1976).
- ¹⁹R. E. de Wames, T. Wolfram, and G. W. Lehman, *Phys. Rev.* 138, A717 (1965).
- ²⁰C. M. Bertoni, V. Bortolani, C. Calandra, and F. Nizzoli, *Phys. Rev. Lett.* 31, 1466 (1973).